Geomechanics and Engineering, Vol. 3, No. 1 (2011) 29-43
DOI: http://dx.doi.org/10.12989/gae.2011.3.1.029

Finite element analysis of a piled footing under horizontal loading

Dj. Amar Bouzid*

Department of Civil Engineering, Engineering Institute,
University Yahia Fares of Médéa, Quartier Ain D´Hab, Médéa 26000, Algeria

(Received August 3, 2009, Accepted November 19, 2010)

Abstract. In this paper a semi-analytical approach is proposed to study the lateral behavior of a piled footing under horizontal loading. As accurate computation of stresses is usually needed at the interface separating the footing (pile) and the soil, this important location should be appropriately modeled as zero-thickness joint element. The piled footing is embedded in elastic soil with either homogeneous modulus or modulus proportional to depth (Gibson's soil). As the pile is the principal element in the piled footing system, a limited parametric study is carried out in order to investigate the influence of footing dimensions and the interface conditions on the lateral behavior of the pile. Hence, the pile behavior is examined through its main governing parameters, namely, the lateral displacement profiles, the bending moments, the shear forces and the soil reactions. The numerical results are presented for Poisson's ratio of 0.2 to represent a large variety of sands and Poisson's ratio of 0.5 to represent undrained clays.

Keywords: piled footing; horizontal loading; semi-analytical approach; interface elements; homogeneous and Gibson's soil.

1. Introduction

In recent decades, piled raft foundations have been recognized to be an economical way to enhance the serviceability of foundation performance by reducing settlement to acceptable margins without compromising the foundation safety (Liang *et al.* 2003, Kitiyodom and Matsumoto 2002, 2003). The footing in this system has an adequate bearing capacity and, therefore, the main objective of introducing piles is to control or minimize the average and differential settlements of the pile/footing system, rather than to carry the major portion of the loads. This is probably true for the building foundations, however, for bridges foundations, the piles are the principal elements in the pile/footing system (Rollins and Sparks 2002), and consequently they are required to resist significant lateral forces produced by earthquakes, winds, waves and ship impacts. Although, this type of foundations has been properly designed against vertical loads, little information has been published when lateral loads are concerned. As the footings are often massive and deeply buried, they have the ability to resist lateral loads, which are usually neglected in the design. Neglecting footing resistance can result in excessively conservative estimates of pile deflections and bending

*Corresponding author, Lecturer, Ph.D., E-mail: d_amarbouzid@yahoo.fr

moments, exceeding those of actual behaviour by 100% or more (Mokwa and Duncan 2001).

Even with the availability of highly sophisticated fast computers, the soil/pile interaction problems remain difficult to analyze, especially when piles are connected to a cap and loaded three-dimensionally and they are in a complex configuration.

FE analysis requires precise estimation of stresses along any soil/structure interface. For modeling interfaces in the axisymmetric problems subjected to non-axisymmetric loadings, Amar Bouzid *et al*. (2004) developed a zero thickness interface model based on an accurate analytical stiffness matrix. This model showed excellent results for stresses estimation. Furthermore, it has been employed to analyze an embedded circular footing under horizontal loading in a non-homogeneous soil (Amar Bouzid and Vermeer 2007) and an embedded disc under prescribed displacements (Amar Bouzid and Vermeer 2009).

By modeling the contact between the piled footing and soil by means of interface elements previously developed (Amar Bouzid *et al*. 2004), this paper presents a limited parametric study in which the effect of footing dimensions along with the interface conditions on the lateral behavior of the pile has been examined. Hence, the influence of interface smoothness and roughness as well as the Poisson's ratio on the variation of pile lateral displacement profiles, the pile bending moments, the shear forces and the soil reactions are thoroughly investigated.

2. Semi-analytical finite element formulation

The analysis of an embedded circular footing connected to a vertical pile under horizontal loading falls into the category of semi-analytical techniques. This class of problems is characterized by a three-dimensional structure in which the geometry exhibits axial symmetry and the loading is non-axisymmetric. Furthermore, the material properties are kept unchanged in the circumferential direction, but the applied load may be dependent on this coordinate. The semi-analytical approach involves expressing forces and all pertinent field variables in the direction of revolution as a Fourier series, thus reducing the analysis to a series of uncoupled two-dimensional analyses (Wilson 1965, Winnicki and Zienkiewicz 1979, Smith and Griffiths 1988, Taiebat and Carter 2001, Zienkiewicz and Taylor

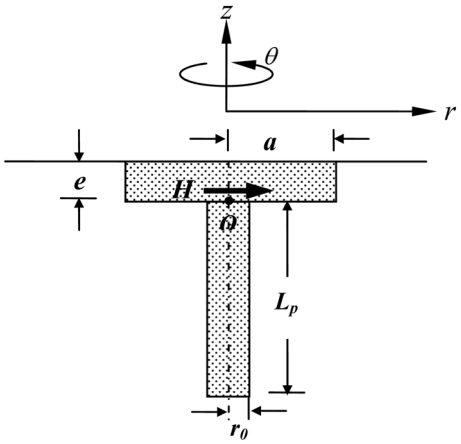

Fig. 1 Embedded piled footing under lateral loading

2001). The semi-analytical procedure will be more efficient than a full 3-D analysis, provided that the loading may be represented by a reasonable number of harmonics. For full details about the semi-analytical method the reader is referred to the above cited references.

The problem of an embedded piled footing (Fig. 1) is a 3D problem, in the sense that all the three displacement components are in general nonzero. Similarly, all six stress components are in general nonzero.

Fig. 1 shows an embedded piled footing subjected to a horizontal load acting at a reference point O, which stands for the connection between the pile and the footing. $\boldsymbol{a}$ is the footing radius, $\boldsymbol{e}$ the footing embedment, r_0 the pile radius and L_p is the pile length.

2.1 Strain and displacement fields

As the problem concerned with the solid of revolution has geometric symmetry (Fig. 1), it is convenient to adopt a cylindrical coordinate system for the finite element formulation. The six strain components may be related to three displacement components which are the radial displacement u, the axial displacement v, and the circumferential displacement w. For the strains it yields

$$\varepsilon_r=\frac{\partial u}{\partial r};\ \ \varepsilon_z=\frac{\partial v}{\partial z};\ \ \varepsilon_\theta=\frac{\partial w}{r\partial\theta}+\frac{u}{r}$$
$$\gamma_{rz}=\frac{\partial u}{\partial z}+\frac{\partial v}{\partial r};\ \ \gamma_{z\theta}=\frac{\partial v}{r\partial\theta}+\frac{\partial w}{\partial z};\ \ \gamma_{\theta r}=\frac{\partial u}{r\partial\theta}+\frac{\partial w}{\partial r}-\frac{w}{r} \tag{1}$$

Where, r is the radius, θ is the angle in the circumference direction and z is the vertical coordinate. Following the standard procedure of Fourier series representation one can write

$$u_r=\sum_{i=0}^{L}\bar{u}_{ri}\cos i\theta+\sum_{i=1}^{L}\bar{\bar{u}}_{ri}\sin i\theta$$
$$v_z=\sum_{i=0}^{L}\bar{v}_{zi}\cos i\theta+\sum_{i=1}^{L}\bar{\bar{v}}_{zi}\sin i\theta \tag{2}$$
$$w_\theta=\sum_{i=1}^{L}\bar{w}_{\theta i}\sin i\theta+\sum_{i=0}^{L}\bar{\bar{w}}_{\theta i}\cos i\theta$$

Where, each term of each series is called a harmonic. The single barred terms $\bar{u}_{ri}$, $\bar{v}_{zi}$, $\bar{w}_{\theta i}$ are amplitudes of displacements that are symmetric with respect to the plane for $\theta=0$. The double barred terms $\bar{\bar{u}}_{ri}$, $\bar{\bar{v}}_{zi}$, $\bar{\bar{w}}_{\theta i}$ are the amplitudes of displacements that are antisymmetric with respect to the plane for $\theta=0$. The index i indicates the harmonic number, and L is the total number of harmonic terms considered in the series.

2.2 Stress fields

In most practical problems only the first two terms in the Fourier series are needed. Problems for the first term $i=0$ are relevant to purely axisymmetric problems and consequently well established in the literature. The second term for $i=1$ is required when the loading pattern has a plane of symmetry. In this situation the components of displacement will reduce to

$$u_r = \bar{u}_r \cos\theta, \quad v_z = \bar{v}_z \cos\theta, \quad w_\theta = \bar{w}_\theta \sin\theta \tag{3}$$

The strains and stresses calculated at the Gauss points are themselves amplitudes. The actual values of stresses at various tangential locations are therefore found from the relationships

$$\begin{aligned} \sigma_r &= \bar{\sigma}_r \cos\theta, \quad & \tau_{rz} &= \bar{\tau}_{rz} \cos\theta \\ \sigma_z &= \bar{\sigma}_z \cos\theta, \quad & \tau_{z\theta} &= \bar{\tau}_{z\theta} \sin\theta \\ \sigma_\theta &= \bar{\sigma}_\theta \cos\theta, \quad & \tau_{\theta r} &= \bar{\tau}_{\theta r} \sin\theta \end{aligned} \tag{4}$$

Where the barred terms are the computed amplitudes. Similar expressions exist for the six components of strain.

Although more work and storage are required than for a genuine 2D analysis, the fact that finite element discretisation is only required in radial plane means that band-width problems that occur with 3D elements are avoided. Thus the problem is easier for the analyst and is less demanding when considering computer resources.

2.3 Modeling the interface between the piled footing and soil

For many soil/structure interaction problems it may be useful to model interface behavior by simply refining the finite element mesh in the immediate vicinity of the interface. However, significant occasional errors and numerical singularities may occur due to the considerable difference properties assigned to adjacent elements. This probably undermines the use of a refined mesh.

A joint element, based on the idea of a zero-thickness, was formulated to model soil/structures interfaces of axisymmetric solids of revolution subjected to non-axisymmetric loading. Hence, a six-noded interface element was established which can be combined with eight or nine-noded quadrilateral volume elements (Fig. 2). A brief outline of the interface formulation will be given.

According to the standard formulation of the displacement-based finite element method (Cook *et al*. 2001), the stiffness matrix $\boldsymbol{K}_i$ of the interface element is given by the equation

$$\boldsymbol{K}_i = \int_A \boldsymbol{B}^T \boldsymbol{D} \boldsymbol{B} dA \tag{5}$$

Where, $\boldsymbol{B}$ is the strain-displacement matrix, $\boldsymbol{D}$ is the constitutive matrix and A is the area of the

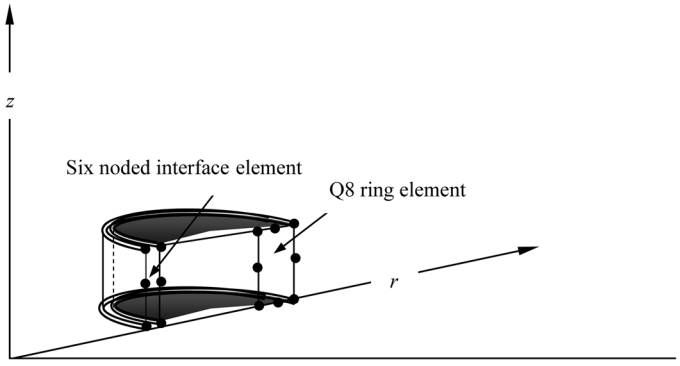

Fig. 2 Zero thickness 6-noded interface element in an axisymmetric body modeled by Q8 ring isoparametric elements

interface element. The thickness of the interface element is taken to be zero.

The interface represents only the interaction between two dissimilar materials, as it is an imaginary location and is not a material itself. Hence, there will exist only a normal stress σ_{ni}, and shear stresses τ_{sni} and $\tau_{n\theta i}$ in this fictitious surface. The displacement-stress relationships can be written as

$$\boldsymbol{\sigma_i} = \boldsymbol{D}\boldsymbol{u_{rel}} \tag{6}$$

Where, $\sigma_i = \begin{Bmatrix} \tau_{sni} \\ \sigma_{ni} \\ \tau_{n\theta i} \end{Bmatrix}$, $\boldsymbol{D} = \begin{bmatrix} k_s & 0 & 0 \\ 0 & k_n & 0 \\ 0 & 0 & k_s \end{bmatrix}$ and $\boldsymbol{u}_{rel} = \boldsymbol{B}\bar{\boldsymbol{u}}^e$

k_s is the interface shear stiffness and k_n is the interface normal stiffness in units of force per cube length. $\bar{\boldsymbol{u}}^e = [\bar{u}_1, \bar{v}_1, \bar{w}_1, ..., \bar{u}_6, \bar{v}_6, \bar{w}_6]^T$ is the vector of radial, axial and tangential nodal displacement amplitudes in the global coordinate system.

As most interface stiffness matrices are formed using numerical integration, the present analytical formulation has the advantage of avoiding spurious oscillations of stresses over the interface as they are accurately determined.

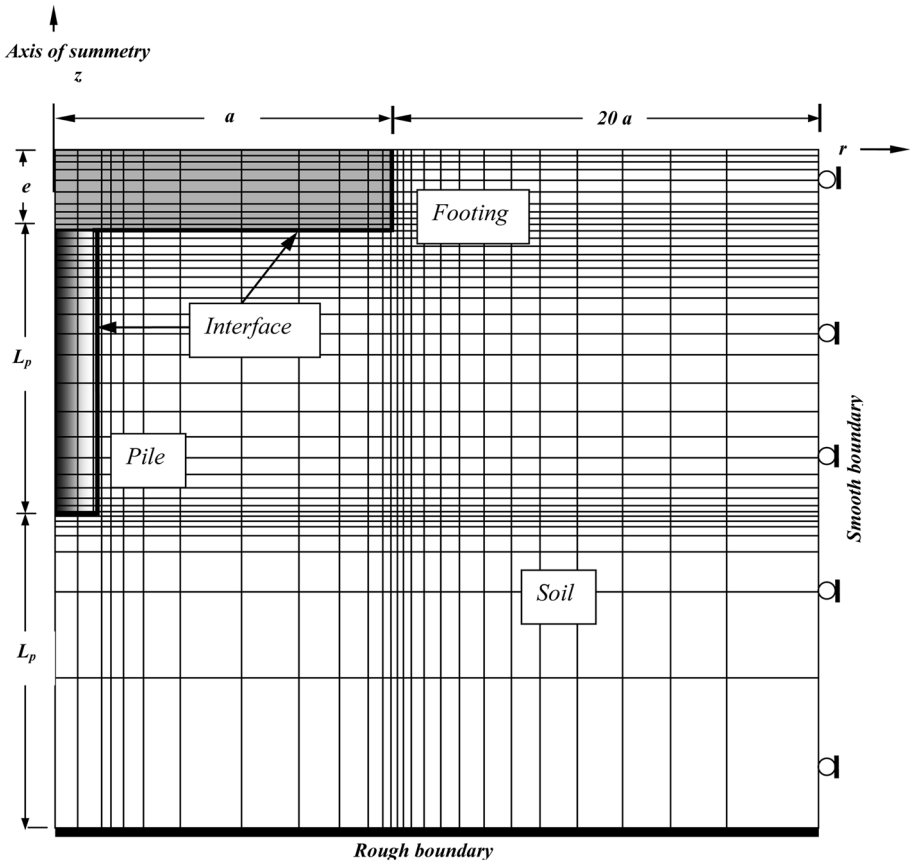

Fig. 3 Finite element mesh of a piled footing

2.4 Finite element mesh

The mesh used for the analysis is depicted in Fig. 3. It consists of using the eight-noded quadrilateral element for modeling both soil and the piled footing system. This element performs well in analyzing problems involving flexural behavior. Furthermore, this element is sufficiently accurate, as it possesses a quadratic field of displacements, which is suitable for problems characterized by flexural behaviour (Durocher *et al.* 1978).

The mesh is relatively fine around the footing and the pile, in order to ensure accuracy of displacements and consequently stresses at the interface. The elements increase progressively in size with growing distance to the footing. Both a rough and smooth piled footing will be considered. The smooth case is modeled by introducing interface elements as also indicated in Fig. 3. The normal interface stiffness is given a large value $k_n = 10^{10}$ (kN/m^3), so that the interface is hardly compressed (Amar Bouzid *et al.* 2004) and the shear stiffness k_s is simply set to zero.

The rough interface between the piled footing and the surrounding soil has been simulated by either prescribing large values for interface stiffnesses ($k_n = 10^{10}$ kN/m^3 and $k_s = 10^{10}$ kN/m^3) or removing completely the interface formulation from the finite element code by using a conventional finite element analysis in which soil and the structure are tied together at the shared nodes.

It is worth noting here that owing to the elastic nature of the interface constitutive model, the deformation process should not allow for the appearance of gaps between the piled footing and soil.

3. Parametric study: Effect of interface conditions and footing dimensions on pile behavior in the piled footing system

The pile in the piled footing system might represent in the majority of cases the equivalent of a group of piles. It is sometimes a single pile in the case of certain spread footings where the pile is added when one fears excessive settlements of the footing.

As far as the influence of the footing on the lateral behavior of the pile is concerned, it appeared useful to consider the reference-line of the horizontal force H at the point O (Fig. 1).

Since the factors affecting the lateral behavior of a piled footing are numerous and they are difficult to handle in a single analysis, the objective of this study is to identify a limited number of them being able to influence the behavior of the pile like footing dimensions and the state of the interfaces. Indeed, we focus on the study of the influence of these factors on the principal parameters governing the behavior of the pile, namely: profiles of lateral displacements, bending moments, shear forces and the soil reactions. Three ratios of footing radius, $a/e = 1$, $a/e = 3$ and $a/e = 6$ have been chosen. This will probably cover a wide range of footing applications whose diameters are in general less than 12 m with an embedment of 1 m. Two pile slendernesses $L_p/d = 10$ and $L_p/d = 25$ have been selected along with two Poisson's ratios $v_s = 0.2$ et $v_s = 0.5$ to represent respectively a large variety of sands (Lade 1977) and undrained clays. For the second case, a value of $v_s = 0.499$ has been used in the computations instead of 0.5 in order to avoid stiffness singularities. Both rough and smooth interfaces have been considered in this study. In the smooth case, the normal interface stiffness is given a large value, so that this interface is hardly compressed, and the shear stiffness is simply set to zero.

3.1 Piled footing in a homogeneous soil

Firstly semi-analytical computations have been carried out in a homogeneous soil characterized by a constant soil/pile relative stiffness $E_p/E_s = 1000$ with E_p pile Young's modulus ($E_p = 30.10^6$ KN/m^2). The footing and pile Poisson's ratios are respectively $v_f = 0.15$ and $v_p = 0.25$.

Results of analysis for the case of homogeneous soil have been reported in Figs. 4-11. These figures show the profiles of pile lateral deflection, bending moments, shear forces and soil pressure in function of normalized depth (z/L_p), where L_p is the pile length. The ordinate origin has been taken at point O, corresponding to the pile head.

3.1.1 Normalized displacements

Non-dimensional displacement uE_sd/H is plotted in Figs. 4 and 5 respectively for slenderness $L_p/d = 10$ and $L_p/d = 25$. The first observation which will be generalized later for the other parameters, is that displacement is less important as the footing radius ratio is larger. This is obviously what would be expected (Poulos and Davis 1980). On another hand, the interface state shows a

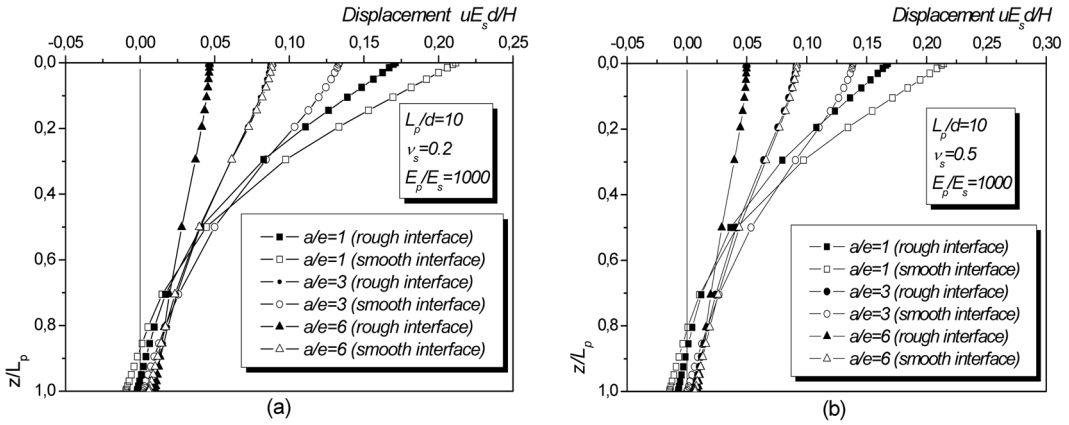

Fig. 4 Pile lateral deflection, piled footing embedded in a homogeneous soil: (a) $v_s = 0.2$, (b) $v_s = 0.5$

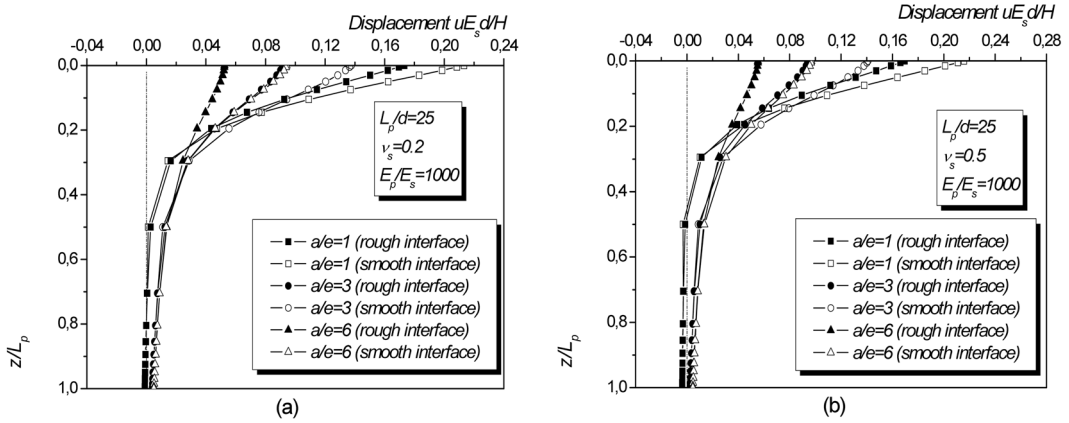

Fig. 5 Pile lateral deflection, piled footing embedded in a homogeneous soil: (a) $v_s = 0.2$, (b) $v_s = 0.5$

tremendous effect on the lateral behavior of the pile. It is clearly seen that the interface smoothness increases considerably the magnitude of displacement. In contrast, the interface roughness reduces the lateral deflections at the pile head. If the whole pile length of slenderness $L_p/d = 10$ is affected by displacements, only the upper part of pile length of slenderness $L_p/d = 25$ undergoes important displacements. This is probably due to the nature of piles selected in this study, which are respectively rigid and flexible with respect to the pile/soil stiffness adopted in this work.

3.1.2 Normalized bending moment

The variation of bending moments M/Hd with respect to relative depth is plotted in Figs. 6 and 7 for the two slenderness ratios. At a close examination of these figures, we realize first that negative moments appear at the head of piles because of the rigid connection of the pile with the embedded footing. If negative moments at the head are very close in values, the maximum positive moments which appear in depth are very influenced by the footing radius ratio a/e and the state of interface. Indeed, the smaller a/e gets, the greater the maximum bending moment becomes as the interface is

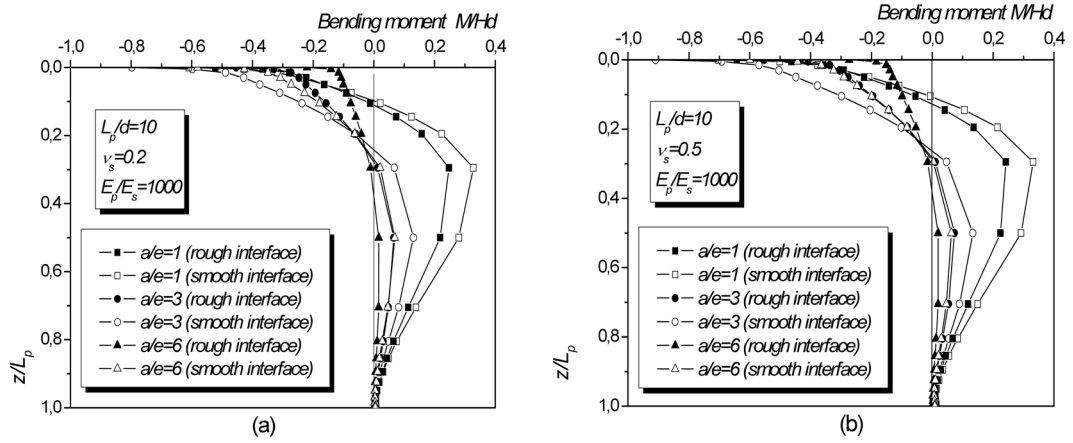

Fig. 6 Pile bending moment, piled footing embedded in a homogeneous soil: (a) $v_s = 0.2$, (b) $v_s = 0.5$

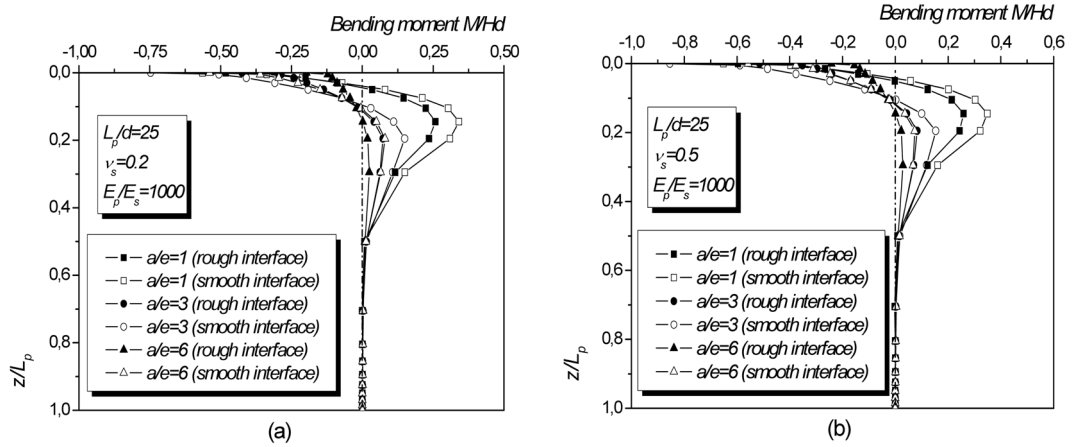

Fig. 7 Pile bending moment, piled footing embedded in a homogeneous soil: (a) $v_s = 0.2$, (b) $v_s = 0.5$

smooth. It might be worthwhile to point out that the location of the maximum positive moment moves downwards when a/e increases.

3.1.3 Normalized shear forces

The distribution of normalized shear forces T/H with relative depth z/L_p is illustrated in Figs. 8 and 9 for the two slenderness ratios in homogeneous soil.

We notice first, that the shearing action propagates over the entire length of the short pile, whereas only the upper half of the slender pile undergoes shear forces. Furthermore, the smaller the footing radius ratio a/e gets, the more significant the shear forces become. In particular, Fig. 8 shows clearly the tremendous effect of the interface state on the values of shear forces at pile heads. In deed, the greater the footing radius ratio is, the more important the difference between a rough and a smooth interface becomes.

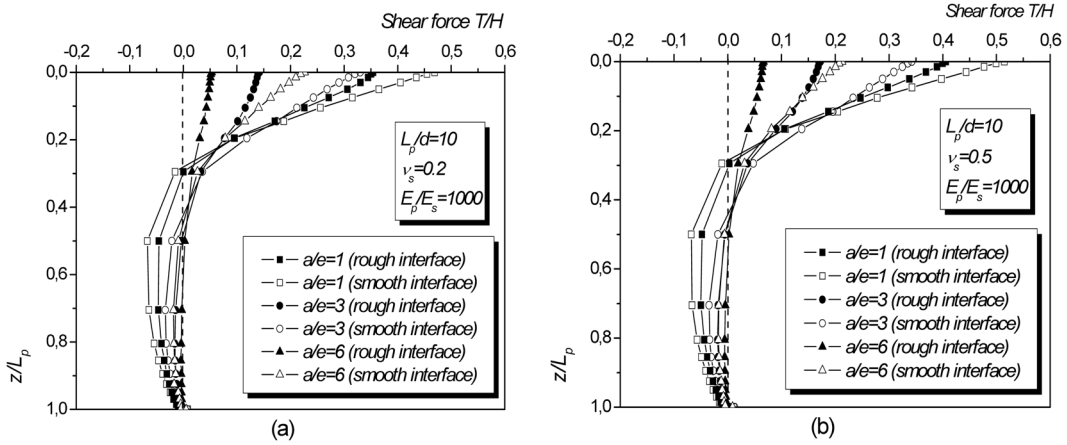

Fig. 8 Shear forces along the pile shaft, piled footing embedded in a homogeneous soil: (a) $\nu_s = 0.2$, (b) $\nu_s = 0.5$

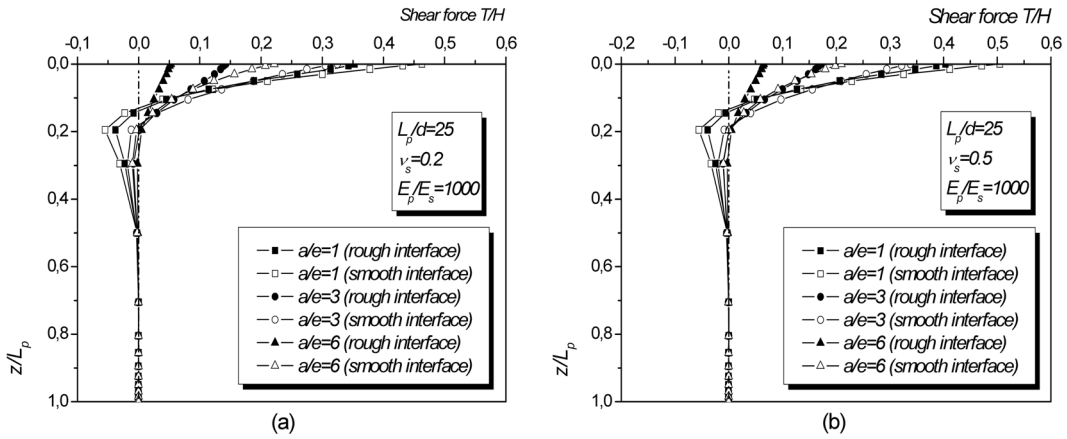

Fig. 9 Shear forces along the pile shaft, piled footing embedded in a homogeneous soil: (a) $\nu_s = 0.2$, (b) $\nu_s = 0.5$

3.1.4 Normalized soil reaction

Variation of normalized soil reaction Pd/H in function of relative depth is presented in Figs. 10 and 11. The first thing we can notice from these figures, is the important differences between short and long piles when soil reaction is considered. Hence, while the entire length of short piles mobilizes soil reaction, only the upper one fourth (1/4) of slender piles can really receive soil pressure.

3.2 Piled footing in a Gibson's soil

In addition to homogeneous soil, a Gibson's soil has been also considered. This type of soils is characterized by an elasticity modulus which varies linearly with depth ($E_s = mz$, m is the rate of increase with depth). The soil/pile relative stiffness selected for this parametric study is: $E_p/E_{se} = 1000$, where E_{se} is the soil modulus at the level of footing base. The same elasticity modulus has been attributed to the footing (E_p/E_c=1) with a footing Poisson's ratio of $\nu_f = 0.15$.

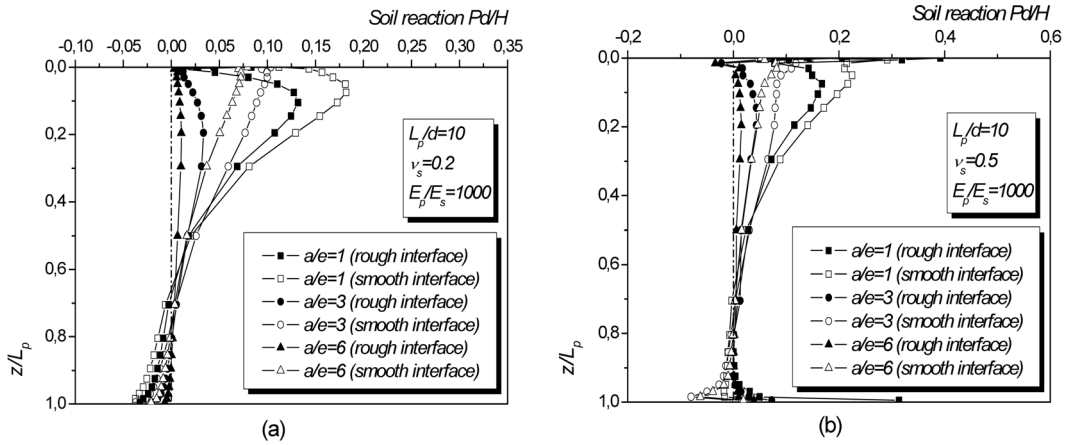

Fig. 10 Soil reaction along the pile shaft, piled footing embedded in a homogeneous soil: (a) $\nu_s = 0.2$, (b) $\nu_s = 0.5$

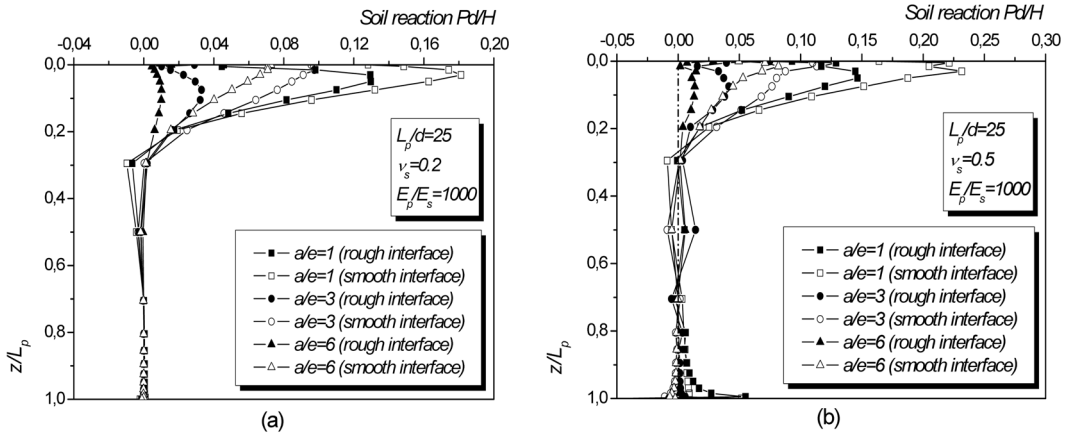

Fig. 11 Soil reaction along the pile shaft, piled footing embedded in a homogeneous soil: (a) $\nu_s = 0.2$, (b) $\nu_s = 0.5$

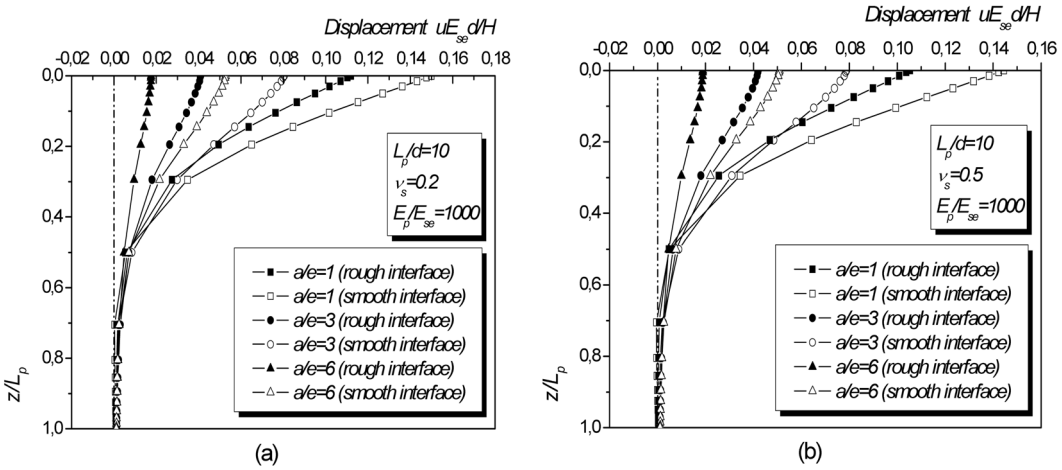

Fig. 12 Pile lateral deflection, piled footing embedded in a Gibson's soil: (a) $v_s = 0.2$, (b) $v_s = 0.5$

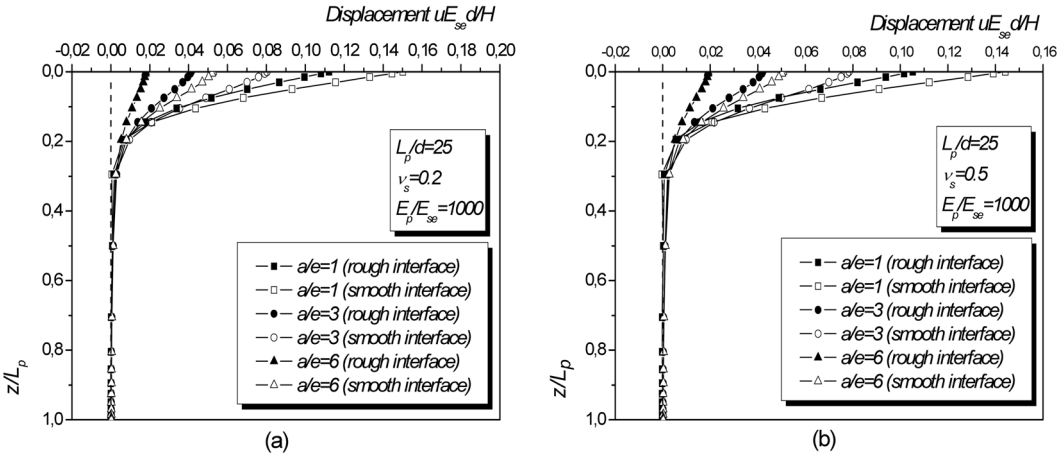

Fig. 13 Pile lateral deflection, piled footing embedded in a Gibson's soil: (a) $v_s = 0.2$, (b) $v_s = 0.5$

Results of numerical computations for a piled footing under horizontal loading and embedded in a Gibson's soil are illustrated in Figs. 12-19.

The variation of normalized displacements with relative depth is shown on Figs. 12 and 13. Although, negative displacements at the bottom of short piles ($L_p/d = 10$) have been clearly noticed for the case of homogeneous soil, lateral displacements of short piles are approximately zero at the bottom for this type of piles in Gibson's soil. This means that the latter absorbs negative displacements.

The distribution of normalized bending moments M/Hd with respect to relative depth is plotted in Figs. 14 and 15 for the two slenderness ratios considered in this study, and for the cases of $v_s = 0.20$ and $v_s = 0.50$. Three important points can be worth noting from the examination of this bending moment distribution. Firstly, the global trend is the same as what has been observed in the homogeneous soil case with slight differences for slender piles. Secondly, a close examination of the Fig. 14, shows that no bending moment occurs in the lower quarter pile length, whereas the whole

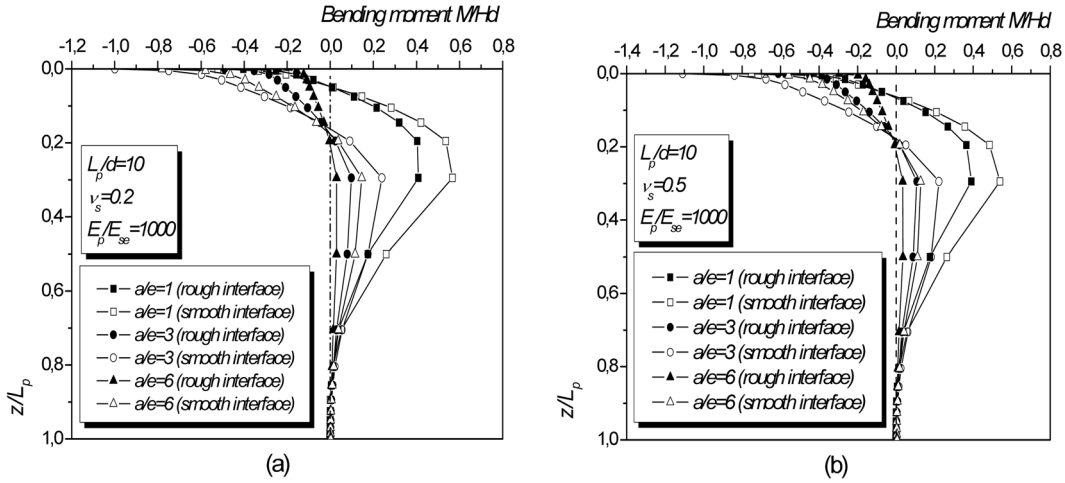

Fig. 14 Bending moment along the pile shaft, piled footing embedded in a Gibson's soil: (a) $\nu_s = 0.2$, (b) $\nu_s = 0.5$

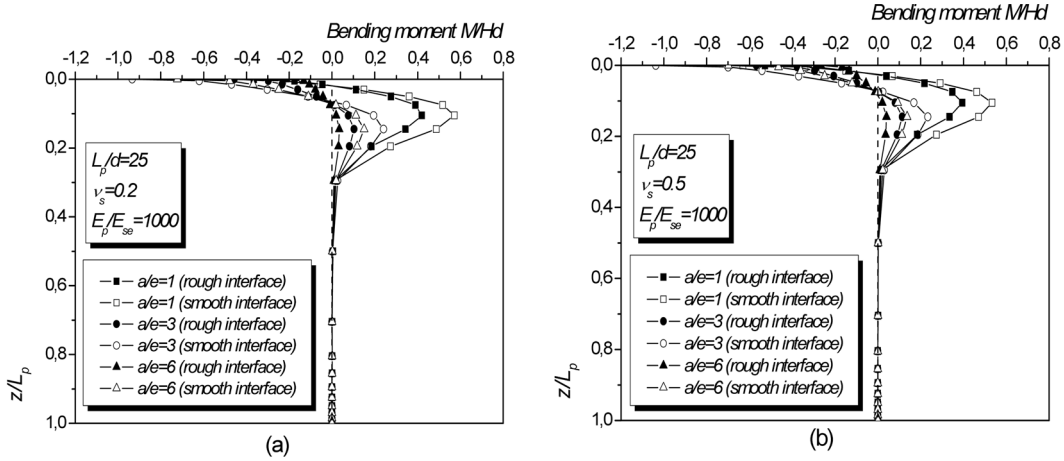

Fig. 15 Bending moment along the pile shaft, piled footing embedded in a Gibson's soil: (a) $\nu_s = 0.2$, (b) $\nu_s = 0.5$

pile length undergoes bending moment when embedded in a homogeneous soil. Thirdly, the distribution of moments with depth in Fig. 15 (slender piles), shows, that only the upper one fifth (1/5) of pile length is subjected to bending moment. This means that, Gibson's soil reduces significantly the magnitude of bending moments.

The evolution of shear forces T/H with relative depth z/L_p is illustrated in Figs. 16 and 17.

The same remarks observed for bending moments can be done for shear forces. The important differences are observed for slender piles. The maximum negative shear force moves upward in Gibson's soil and only the upper third of slender pile length undergoes shear forces when embedded in this type of soil.

Figs. 18 and 19 illustrate the variation of normalized soil reaction Pd/H with respect to relative

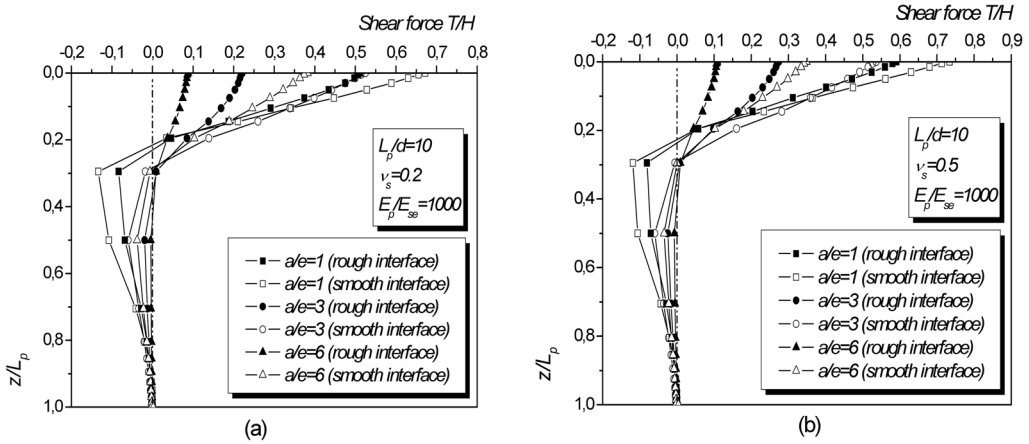

Fig. 16 Shear forces along the pile shaft, piled footing embedded in a Gibson's soil: (a) $v_s = 0.2$, (b) $v_s = 0.5$

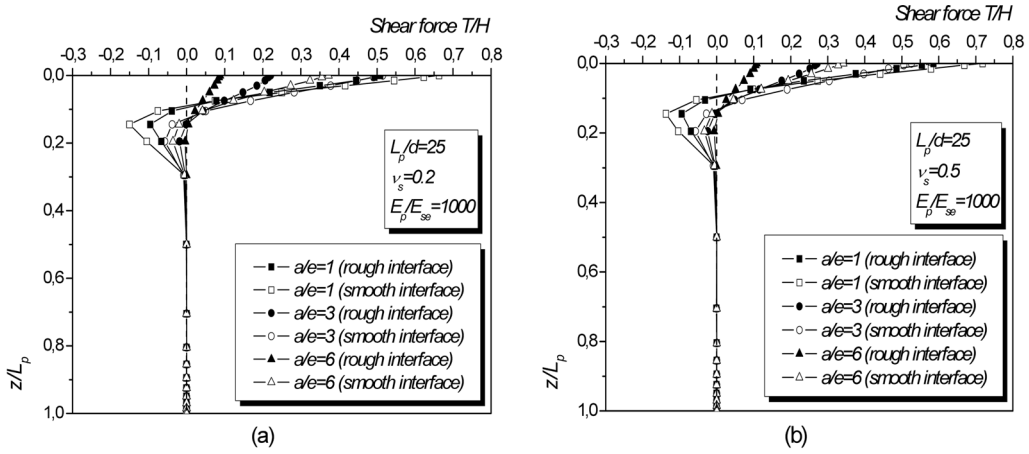

Fig. 17 Shear forces along the pile shaft, piled footing embedded in a Gibson's soil: (a) $v_s = 0.2$, (b) $v_s = 0.5$

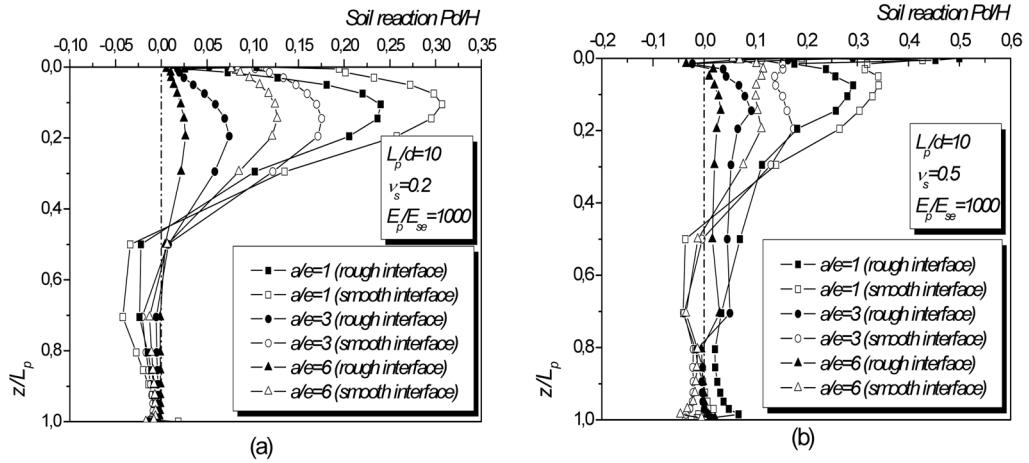

Fig. 18 Soil reaction along the pile shaft, piled footing embedded in a Gibson's soil: (a) $v_s = 0.2$, (b) $v_s = 0.5$

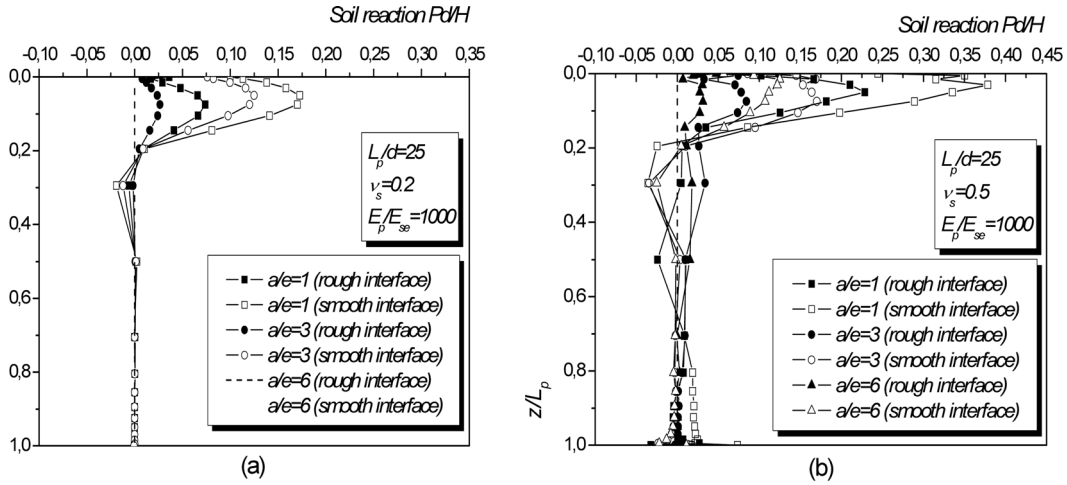

Fig. 19 Soil reaction along the pile shaft, piled footing embedded in a Gibson's soil: (a) $\nu_s = 0.2$ (b) $\nu_s = 0.5$

depth. These figures show that short piles ($L/d = 10$) behave in a completely different manner in Gibson's soil than that in homogeneous soil. In the latter, we have seen that a short pile rotates about a point situated near its tip, but in a non-homogeneous soil the pile undergoes flexion in its lower part. The same remarks as those done for slender piles in homogeneous case can be drawn here.

4. Conclusions

The addition of a footing to a vertical pile is the current practice in the majority of the foundations of the structures. Although the design of this type foundations with respect to the vertical loads is well mastered, few information are available when horizontal loads are considered and studies relevant to this type of loading are rare in the literature.

An embedded circular footing connected to a vertical pile under horizontal loading is a soil/structure interaction problem, which belongs to the class of problems where the loading is arbitrary in nature and the geometry is axisymmetric. Consequently, the finite element semi-analytical approach has been used in the present investigation to analyze the piled footing under horizontal H loading. When compared to general 3-D analyses the semi-analytical approach has some advantages.

A limited parametric study involving a piled footing in both homogeneous and non-homogeneous soil with various soil/pile stiffnesses has been carried out. Both rough and smooth interfaces have been considered in the parametric study.

This work made it possible to quantify the effect of footing dimensions and state of interfaces on the lateral behavior of the pile to which the footing is added. Indeed, lateral displacements, bending moments, shear forces and soil reactions showed a great dependence on the interface conditions as well as on the footing radius.

References

Amar Bouzid, Dj., Tiliouine, B. and Vermeer, P.A. (2004), "Exact formulation of interface stiffness matrix for axisymmetric bodies under non-axisymmetric loading", *Comput. Geotech.*, **31**(2), 75-87.

Amar Bouzid, Dj. and Vermeer, P.A. (2007), "Effect of interface characteristics on the influence coefficients of an embedded circular footing under horizontal and moment loading", *Geotech. Geo. Eng.*, **25**, 487-497.

Amar Bouzid, Dj. and Vermeer, P.A. (2009), "Fourier series based FE analysis of a disc under prescribed displacements-elastic stress study", *Arch. Appl. Mech.*, **79**(10), 927-937.

Cook, R.D., Malkus, D.S., Plesha, M.E. and Witt, R.J. (2001), *Concepts and applications of finite element analysis*, 4th edn., London, Wiley.

Durocher, L.A., Gasper, A. and Rhoades, G. (1978), "A numerical comparison of axisymmetric finite elements", *Int. J. Numer. Meth. Eng.*, **12**, 1415-1427.

Kitiyodom, P. and Matsumoto, T. (2002), "A simplified analysis method for piled raft and pile group foundations with batter piles", *Int. J. Numer. Anal. Meth. Geomech.*, **26**, 1349-1369.

Kitiyodom, P. and Matsumoto, T. (2003), "A simplified analysis method for piled raft foundations in non-homogeneous soils", *Int. J. Numer. Anal. Meth. Geomech.*, **27**, 85-109.

Lade, P.V. (1977), "Elasto-plastic stress-strain theory for cohesion-less soil with curved yield surface", *Int. J. Solids Struct.*, **13**, 1019-1035.

Liang, F.Y., Chen, L.Z. and Shi, X.G. (2003), "Numerical analysis of composite piled raft with cushion subjected to vertical load", *Comput. Geotech.*, **30**, 443-453.

Mokwa, R.L. and Duncan, J.M. (2001), "Evaluation of lateral-load resistance of pile caps", *J. Geotech. Geoenviron. Eng.*, **127**(2), 185-192.

Poulos, H.G. and Davis, E.H. (1980), *Pile foundation analysis and design*, Wiley, New York,

Rollins, K.M. and Sparks, A. (2002), "Lateral resistance of full-scale pile cap with gravel backfill", *J. Geotech. Geoenviron. Eng.*, **128**(9), 711-723.

Smith, I.M. and Griffiths, D.V. (1988), *Programming the finite element method*, 2nd ed. John Wiley and Sons, Chichester.

Taiebat, H.A. and Carter, J.P. (2001), "A semi-analytical finite element method for three-dimensional consolidation analysis", *Comput. Geotech.*, **28**, 55-78.

Wilson, E.L. (1965), "Structural analysis of axisymmetric solids", *J. Am. Inst. Aeronaut. Astronaut.*, **3**(12), 2269-2274.

Winnicki, L.A. and Zienkiewicz, O.C. (1979), "Plastic (or visco-plastic) behavior of axisymmetric bodies subjected to non-axisymmetric loading-semi-analytical-finite element solution", *Int. J. Numer. Meth. Eng.*, **14**, 1399-1412.

Zienkiewicz, O.C. and Taylor, R.L. (2001), *The finite element method*, 4th edn., London McGraw-Hill.

PL